J. CHEM. SOC. FARADAY TRANS., 1991, 87(21), 3473–3478

Study of the Temperature Dependence of the Reaction of the Nitrate Radical with Propene

Carlos E. Canosa-Mas, Stuart J. Smith, Steven J. Waygood and Richard P. Wayne*
Physical Chemistry Laboratory, University of Oxford, South Parks Road, Oxford OX1 3QZ, UK

Rate constants have been determined for the reaction of NO_3 with propene from room temperature up to $T = 553$ K. Allowance was made in analysing experimental data for probable secondary reactions. The Arrhenius plot shows some curvature at the higher temperatures, which we suggest can be explained by the abstraction of an allylic H atom followed by chain reactions involving fast radical–radical processes. The rate constant at $T = 298$ K was found to be $(0.93 \pm 0.12) \times 10^{-14}$ cm^3 $molecule^{-1}$ s^{-1}. We propose the following Arrhenius expression, in units of cm^3 $molecule^{-1}$ s^{-1}, for the addition step in the temperature range $T = 298$–423 K

$$k = (2.04^{+0.78}_{-0.55}) \times 10^{-13} \exp[-(943 \pm 108)/T].$$

For the abstraction reaction of an allylic H atom, we present arguments that suggest Arrhenius parameters of $A = 6.8 \times 10^{-13}$ cm^3 $molecule^{-1}$ s^{-1} and $E = 18$ kJ mol^{-1}.

Reactions of the nitrate radical are of importance in the night-time troposphere. Such reactions contribute significantly to the losses of several types of volatile organic compound, and represent the major oxidation route for many unsaturated organic species, including natural hydrocarbons. The radical is a key intermediate[1] in the formation of nitric acid, which is formed either by hydrolysis of N_2O_5 (resulting from the combination of NO_2 with NO_3) or by abstraction by NO_3 of an H atom from an organic species.

There have been previous determinations[2–4] of the rate of reaction of propene with NO_3 at room temperature, but our work is the first direct, discharge-flow investigation and also the first to study the temperature dependence of the reaction. We shall show that the Arrhenius plot exhibits some nonlinearity at the highest temperatures employed ($T = 473$ and 523 K) and we suggest that the most likely explanation is a chain reaction initiated by the abstraction of an allylic hydrogen by the NO_3 radical.

Since tropospheric mixing ratios of propene as high as several ppb have been measured at different altitudes and latitudes,[5,6] a more comprehensive study of the reactivity of this compound with NO_3 is clearly desirable for a better understanding of the urban night-time troposphere.

Experimental

The discharge-flow system and the multipath optical absorption cell for the measurement of $[NO_3]$ at $\lambda = 662$ nm have already been described.[7,8] The nitrate radical was generated by the reaction

$$F + HNO_3 \rightarrow NO_3 + HF \tag{1}$$

and the flow technique provides time resolution and hence absolute rate constants. The flow tube was heated by an electronically regulated electric oven that provided temperatures between room temperature and 553 K. The entrance region of the flow tube, upstream of the electrical oven, was heated by a small resistance-oven controlled separately from the main oven in order to preheat all the gases entering the flow tube and to avoid a drop of temperature at the end of the main oven. At the end of the flow tube where the absorption cell is situated, such arrangement is not possible in our system. The temperature difference thus has to be taken into consideration in the evaluation of the rate coefficients. The injection ports were situated at 19.5, 44.0, 70.1 and 95.1 cm from the centre of the observation region, giving contact times in the region 60–320 ms. In a previous study,[7] we saw no dependence of the reaction rate on pressure over the approximate range 0.6–12 mmHg for the reactions of NO_3 with ethene, ethyne, propyne, but-1-yne or but-2-yne. No pressure effect is therefore expected for the reaction of NO_3 with propene, and all the experiments were carried out at a single pressure (2.1 mmHg). The rate constant for wall loss of NO_3 was determined to be less than 0.1 s^{-1} at all temperatures used.

Helium (B.O.C., commercial grade) was passed through an oxygen-removing column ('Oxisorb', Messer Griesheim) and through a trap containing molecular sieve (4A). Fluorine (5% in He, B.O.C. special gases), sulphuric acid (Fisons, 98%) and nitric acid (B.D.H. Aristar, 70%) were used without treatment, except for evacuating the cold acid mixture in order to remove NO_2 present. Propene was obtained from Matheson (C.P. grade, >99%). It was purified by successsive trap-to-trap distillations.

The minimum $[NO_3]$ measurable for a 1 : 1 signal-to-noise ratio and an integration time of 10 s was *ca.* 10^{12} molecule cm^{-3}.

Results and Fitting Procedures

Concentrations of NO_3 were determined as a function of the distance from the point of injection to the centre of the absorption cell. The observed $[NO_3]$ decays were plotted as a function of time. Fig. 1 shows some typical results for reaction of NO_3 with C_3H_6 at room temperature and at 423 K.

As propene is not present in our experiments in a large excess over NO_3, and since the measured losses of NO_3 may still include those resulting from secondary reactions, the experimental data have to be analysed using a numerical kinetic model. Because the question of secondary reactions is so important in interpreting slow reactions studied by the flow technique, we shall discuss them in some detail. In our previous work on the reactions with alkenes and alkynes,[7,8] we found kinetic evidence to support the hypothesis that the NO_3 adds to the double or triple bonds forming a radical adduct which dissociates rapidly to yield NO_2 and an oxide, so that a two-step scheme

$$C_3H_6 + NO_3 \rightarrow C_3H_6O + NO_2 \tag{2}$$

$$NO_2 + NO_3 \rightarrow N_2O_5 \tag{3}$$

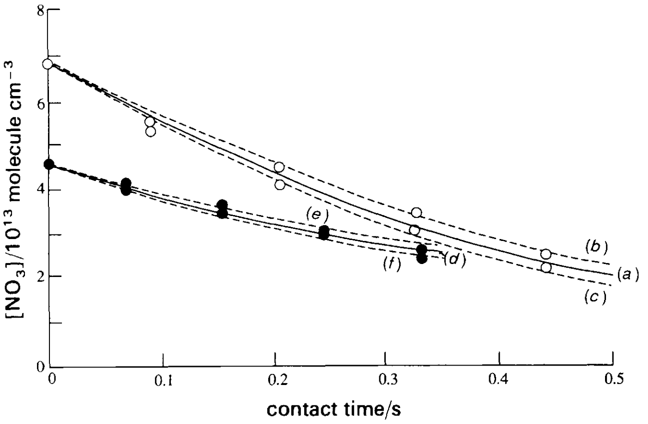

Fig. 1 $[NO_3]$ as a function of contact time for experiments at room temperature and at $T = 423$ K. ○, Experimental $[NO_3]_t$ at $T = 298$ K; $[NO_3]_0 = 6.84 \times 10^{13}$ molecule cm^{-3}; $[C_3H_6]_0 = 1.9 \times 10^{14}$ molecule cm^{-3}; $P = 2.1$ mmHg. Model results with (*a*) $k_2 = 0.96 \times 10^{-14}$ cm^3 molecule^{-1} s^{-1}; (*b*) $k_2 = 0.86 \times 10^{-14}$ cm^3 molecule^{-1} s^{-1}; (*c*) $k_2 = 1.06 \times 10^{-14}$ cm^3 molecule^{-1} s^{-1}. ●, Experimental $[NO_3]_t$ at $T = 423$ K; $[NO_3]_0 = 4.57 \times 10^{13}$ molecule cm^{-3}; $[C_3H_6]_0 = 7.29 \times 10^{13}$ molecule cm^{-3}; $P = 2.2$ mmHg. Model results with (*d*) $k_2 = 2.66 \times 10^{-14}$ cm^3 molecule^{-1} s^{-1}; (*e*) $k_2 = 2.39 \times 10^{-14}$ cm^3 molecule^{-1} s^{-1}; (*f*) $k_2 = 2.93 \times 10^{-14}$ cm^3 molecule^{-1} s^{-1}

operates with our contact times. There now exists direct experimental evidence for the products of the primary step at pressures comparable to those of our studies. First, Dlugokencky and Howard[9] found that, for alkenes with four carbon atoms (*E*-but-2-ene) or less, the yield of NO_2 is unity at low pressure and at room temperature; secondly, Le Bras *et al.* reported[10] that the epoxide is a product in the reaction of NO_3 with tetramethylethylene, and probably also with isoprene. A possible reaction channel leading to propanal seems unlikely because it requires a migration of an H atom.[9]

At elevated temperature, the process

$$N_2O_5 + M \rightarrow NO_2 + NO_3 + M \qquad (4)$$

becomes increasingly important and by $T = 423$ K the concentration of N_2O_5 is negligible.

For use in our numerical model, the value of k_3 at room temperature and at 2.2 mmHg was taken from Smith *et al.*[11] At the higher temperatures, the rate coefficients were calculated using the modified Troe expression recommended in the NASA compilation.[12] The values for k_4 were calculated from k_3 and the equilibrium constant, K_{eq}, given by the equation

$$K_{eq}/\text{cm}^3 \text{ molecule}^{-1} = 6.84 \times 10^{-27} \exp(10815/T) \qquad (I)$$

suggested by Wayne *et al.*[13] We shall show later that this simplified scheme becomes inadequate at the highest temperatures used.

A computer program performed the integration of the differential equations derived from reactions (2), (3) and (4) for a series of values of k_2 which were varied by a given amount (0.01–0.05×10^{-14} cm^3 molecule^{-1} s^{-1}) and it calculated the difference between experimental and modelled NO_3 concentrations. A measure, *D*, of this difference is defined as the square root of the sum of the squares of the differences between the experimental and calculated NO_3 concentrations at each experimental contact time, divided by the total number of experimental points (excluding the initial concentration, which is taken as the starting point of the integration). For each experiment, we take k_2 as the value which gives a minimum in *D*. Table 1 displays these rate coefficients, together with the experimental conditions. Fig. 1 shows the calculated curves for experiments carried out at room temperature and at $T = 423$ K. Also shown are calculated $[NO_3]$ profiles with k_2 taken 10% lower and higher than the chosen value. Table 2 gives some values for the sensitivity, defined as $(\Delta D/D)/(\Delta k_2/k_2)$ for the results at room temperature and at 423 K.

Table 1 Experimental conditions and calculated rate coefficients

	$[NO_3]_0$	$[C_3H_6]_0$	k_2	$k_{2,\text{av}}$
T/K	/10^{13} molecule cm^{-3}		/10^{-14} cm^3 molecule^{-1} s^{-1}	
298	7.07	7.03	1.00	
	7.61	4.61	0.93	
	6.52	6.12	0.84	
	7.77	12.5	0.83	
	7.77	14.5	0.92	0.93 ± 0.12
	7.95	16.8	1.00	
	8.03	17.7	0.90	
	7.81	19.5	0.99	
	6.76	12.8	0.93	
	6.84	19.1	0.96	
333	5.77	6.28	1.21	
	6.16	4.30	1.46	
	6.01	5.38	1.34	1.45 ± 0.36
	5.77	5.40	1.39	
	5.77	2.91	1.60	
	5.66	2.38	1.70	
373	6.43	10.7	1.98	
	7.28	22.9	2.00	
	7.27	10.3	1.92	1.98 ± 0.44
	7.26	6.00	1.66	
	5.39	6.79	1.98	
	5.42	13.3	2.34	
423	4.45	7.10	2.80	
	4.50	11.2	3.21	3.06 ± 0.84
	4.57	7.29	2.66	
	5.69	10.5	3.58	
473	4.01	4.08	4.98	
	3.94	4.90	5.00	
	3.87	5.80	4.86	5.05 ± 0.34
	5.98	9.87	5.30	
	6.07	12.9	5.12	
523	4.89	10.5	8.10	
	4.91	4.87	9.50	9.3 ± 2.4
	4.67	6.59	8.36	
	4.56	2.16	9.24	
	4.90	3.44	11.1	

Error limits are two standard deviations.

For the measurements made above room temperature, some comments are necessary. There is a temperature drop between the position corresponding approximately to the end of the heating elements and the absorption cell, which is not heated. We have measured the temperature profiles as a function of the distance for all temperatures employed in this work with a thermocouple mounted on a sliding probe inserted along the flow-tube axis, using a flow of He under conditions equivalent to that employed in the kinetic experiments. An example of such measurements at $T = 423$ K is shown in Fig. 2. We therefore know the position of the

Table 2 Sensitivity analysis

T/K	$\Delta k_2/k_2$	$\Delta D/D$	$\dfrac{\Delta D}{D}\bigg/\dfrac{\Delta k_2}{k_2}$
298	−0.10	0.53	−5.1
	0.10	0.54	5.1
	−0.21	1.69	−8.1
	0.21	1.40	6.7
423	−0.10	0.73	−7.2
	0.10	0.68	6.7

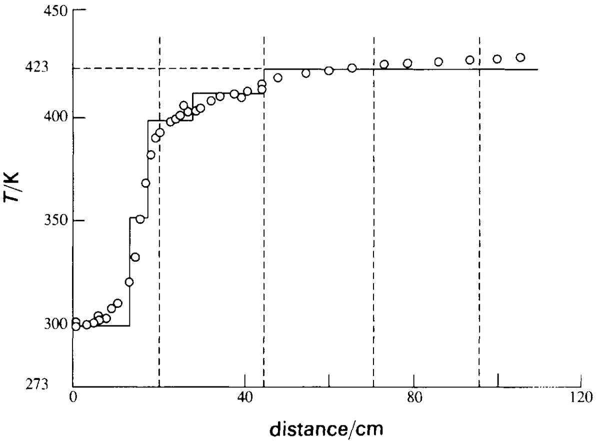

Fig. 2 Temperature profile along the flow-tube axis as a function of the distance from the centre of the absorption cell. ○, Measured temperatures. The solid line shows the temperatures and distances taken for the calculations with the 'step-ladder' model (see text). The vertical broken lines show the position of the injection ports

regions where the temperature is approximately constant and where it falls.

The rate constant, k_2, was determined by performing the model calculation in three different ways. First, we assumed that the entire flow tube was at the same elevated temperature and that the cell was at room temperature. The calculation was carried out for the concentrations of NO_3 corresponding to all the injection ports but the values from the port closest to the cell were given only half the weight of the others. Secondly, we repeated the calculations taking only the NO_3 concentration corresponding to the ports in that part of the flow tube that was approximately isothermal. Thirdly, a 'step-ladder' model with three to six temperatures from the cell to the high (isothermal) temperature region of the reactor was used. The integration was performed from the individual ports to the centre of cell and the calculated NO_3 concentration was then compared with the experimental results. Fig. 2 displays the temperature 'steps' used in the calculations at $T = 423$ K. Only at the highest temperature (523 K) did the values of k_2 calculated using the first method show significant differences from those obtained employing the second and third procedures. Furthermore, the main uncertainties in k_2 at temperatures over 473 K arise from the chemistry rather than from the method of calculation, as we shall discuss shortly. The values in Table 1 for 523 K are those obtained by the second method.

Fortunately, the change in temperature is not so troublesome as it might seem because the increase in reactant concentrations, the decrease in linear flow velocity, and the decrease in k_4 as the temperature is reduced fortuitously compensate for the decrease in the rate constant so that the loss of NO_3 per unit length of the flow tube is approximately the same at all temperatures. In these circumstances, the derived activation energy is much less sensitive to temperature measurements than would be the case if the activation energy were substantially higher or lower. The argument that the calculated activation energy is relatively insensitive to the homogeneity of temperature and the accuracy of its measurement is often stated in relation to processes with zero activation energy, but is erroneous for flow experiments because it does not allow for the influence of temperature on the various physical parameters.

Table 1 shows the rate constants measured at each temperature, and the data are displayed in Fig. 3 in the form of an Arrhenius plot. The value of k_2 at room temperature, $(0.93 \pm 0.12) \times 10^{-14}$ cm^3 molecule^{-1} s^{-1}, is in excellent agreement with the one reported by Atkinson *et al.*[4] of $(0.94 \pm 0.12) \times 10^{-14}$ cm^3 molecule^{-1} s^{-1} determined relative to the rate constant for *E*-but-2-ene $(3.87 \times 10^{-13}$ cm^3 molecule^{-1} s$^{-1})$ at $T = 296$ K and at a pressure of one atmosphere in dry purified air.

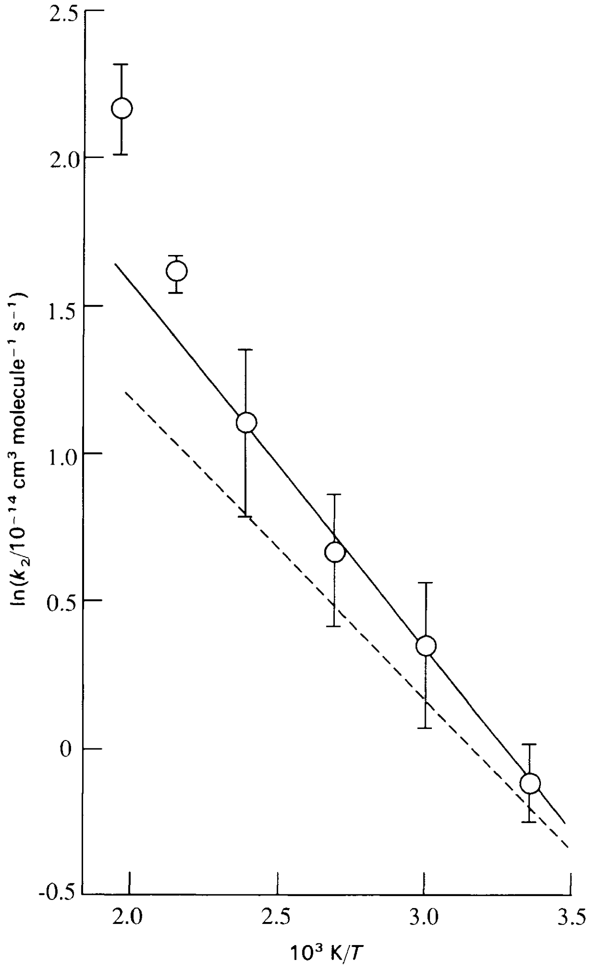

Fig. 3 Arrhenius plot for the reaction of NO_3 with propene. ○, Experimental k_2 from Table 1. Error bars represent two standard deviations. (——) Line calculated using eqn. (II) (*i.e.* with uncorrected values of k_2). (– –) Line calculated with eqn. (IV) (*i.e.* with k_2 corrected for the abstraction process; see text)

A weighted linear least-squares calculation gives an expression, valid between room temperature and $T = 423$ K, of

$$k_2/\text{cm}^3\ \text{molecule}^{-1}\ \text{s}^{-1} = (4.74^{+1.06}_{-0.85}) \times 10^{-13} \exp[-(1171 \pm 66)/T] \quad \text{(II)}$$

corresponding to an activation energy of 9.7 ± 0.8 kJ mol^{-1} (error limits are two standard deviations).

Curvature of the Arrhenius Plot

As shown in Fig. 3, the Arrhenius plot presents a strong upwards curvature above $T = 423$ K. Possible explanations for such curvature include a temperature-dependent pre-exponential factor or the operation of two separate processes for which the activation energies are different. We prefer the second explanation, and discuss next the possible occurrence of an abstraction reaction as well as an addition. We present later our reasons for rejecting the first explanation.

Possible Abstraction of Allylic Hydrogen Atoms

The studies of the products of the reactions of NO_3 with propene and other alkenes[13–15] have usually been carried out at room temperature and at 1 atm pressure in the presence of oxygen, and they indicate that addition to the double bond is the main reaction pathway. However, these studies cannot, by themselves, rule out a contribution from hydrogen abstraction reactions such as

$$CH_2{=}CHCH_3 + NO_3 \rightarrow CH_2{=}CHCH_2 + HNO_3 \quad (5)$$

We have sought ways of estimating reasonable values for a rate constant for hydrogen abstraction, k_5, by analogy with studies of the reactions with OH and $O(^3P)$ of propene and but-1-ene as well as by analogy with the reactivity of NO_3 towards alkanes. A recent review of reactions of the OH radical[16] has summarized the results for the reaction of OH radical with propene. Below 470 K, addition is the main reaction pathway; at room temperature, the contribution from the abstraction of an allylic hydrogen atom is less than 2–5%. These abstraction processes have been the subject of many studies in the reaction of $O(^3P)$ with alkenes, but quantitative conclusions are still lacking. In their review, Cvetanovic and Singleton[17] stated that '… it appears likely that H abstraction from alkenes at room temperature can at best amount only to a few per cent of the total reaction and could be in many cases insignificant'. Kleinermanns and Luntz[18] have studied the nascent OH product-state distribution for the abstraction by $O(^3P)$ from propene, but-1-ene and propyne. They found dynamic thresholds of 6.7, 7.9 and 21 kJ mol^{-1} for the abstraction channel, suggesting that this process occurs more readily in propene than in but-1-ene and with much more difficulty in the reaction with propyne.

In a recent review on the NO_3 radical,[13] a correlation between the logarithm of the rate constant for the abstraction of a hydrogen atom by NO_3 and the bond dissociation energy of the bond being broken was discussed, and the corresponding regression equation calculated. This relationship should not be used directly to estimate rate coefficients when the radical formed by the abstraction has a substantial resonance stabilization energy (which leads to a 'tight' transition state). For the allyl radical, this stabilization energy is *ca.* 50 kJ mol^{-1}. Rossi *et al.*[19,20] treated the stabilization as resonance stiffening of the internal rotation giving a change in the entropy of activation which represents a ten-fold lowering of the *A* factor. The dissociation energy of the allylic hydrogen–carbon bond[21] is 361 kJ mol^{-1}. With this value and the regression equation given in the review, a rate coefficient of *ca.* 5×10^{-15} cm^3 $molecule^{-1}$ s^{-1} for the abstraction of allylic hydrogen atoms can be calculated. Allowing the factor of ten reduction in the *A* factor for radical stabilization, we suggest a rate constant of 5×10^{-16} cm^3 $molecule^{-1}$ s^{-1} at room temperature for the abstraction pathway.

In our earlier work,[22] we measured the activation energies for the reactions of NO_3 with *n*- and iso-butane as 27.0 kJ mol^{-1} and 24.6 kJ mol^{-1}, and the enthalpies of reaction, ΔH_r, are[21] −18.7 and −28.4 kJ mol^{-1}. For the abstraction of the allylic hydrogen ΔH_r is[21] −54.8 kJ mol^{-1}, so that an Evans–Polanyi calculation gives an activation energy for the abstraction of allylic hydrogen of 18 kJ mol^{-1}. Taking $k_5(300\ K) = 5 \times 10^{-16}$ cm^3 $molecule^{-1}$ s^{-1} an Arrhenius expression

$$k_5/cm^3\ molecule^{-1}\ s^{-1} = 6.8 \times 10^{-13} \exp(-18\,000/RT) \quad (III)$$

is obtained for the abstraction channel.

We have recently completed a study of the temperature dependence of the reaction of NO_3 with but-1-ene.[23] It is appropriate to discuss in the present paper the possible abstraction of allylic H atoms from but-1-ene in view of the potential similarity to the propene system. However, the Arrhenius plot for the reaction of NO_3 with but-1-ene is linear up to $T = 473$ K. The dissociation energy for the allylic hydrogen–carbon bond in but-1-ene is[21] 346 kJ mol^{-1}, giving for the reaction

$$CH_2{=}CHC_2H_5 + NO_3 \rightarrow CH_2{=}CHCHCH_3 + HNO_3 \quad (6)$$

an enthalpy change of −73 kJ mol^{-1}. Using the same reasoning as that just advanced for the reaction of NO_3 with propene, an activation energy of 13.4 kJ mol^{-1} can be estimated. The formation of the methylallyl radical involves the freezing of the rotation of two 'heavy' groups (ethyl and vinyl).[24] Thus the *A* factor for the abstraction of one allylic H atom might be less than that for the equivalent reaction of propene. Furthermore, as propene has three allylic H atoms and but-1-ene only two, the contribution from the abstraction channel to the loss of NO_3 might be larger in the case of propene, in agreement with the threshold energies given by Kleinermanns and Luntz.[18]

The possible relevance of the abstraction reaction to the curvature of the Arrhenius plot will now be discussed in some detail. A first approach might be to assume that two processes with different activation energies are operating. A non-linear least-squares fit to a double-exponential expression gives an activation energy of 8.7 ± 0.4 kJ mol^{-1} and a pre-exponential factor of $(3.2 \pm 0.5) \times 10^{-13}$ cm^3 $molecule^{-1}$ s^{-1} for the low-temperature process. However, this approach gives an activation energy for the high-temperature reaction of *ca.* 45 kJ mol^{-1}. This value is much higher than the activation energy just estimated for the abstraction of allylic hydrogen by NO_3. Also, incorporation of reaction (5) into the model calculations with k_5 calculated using eqn. (III) shows that its contribution is not sufficient to explain the increase in the phenomenological rate coefficients at $T = 473$ and 523 K. However, the abstraction of an allylic hydrogen is certainly of importance at the highest temperatures of our study. For an evaluation of the effect of the abstraction at high temperatures we must first consider the stoicheiometry, *s*, for this abstraction channel (*s* is the number of NO_3 molecules lost for each H atom abstracted). We showed in a previous paper[22] that the value of *s* is two (or slightly larger, depending on the experimental conditions) for abstraction of H by NO_3 from alkanes at room temperature. A similar value of *s* should be expected here because, as the addition of the allyl radical to propene is slow (rate constant *ca.* 10^{-17} cm^3 $molecule^{-1}$ s^{-1}), the allyl radical formed in reaction (5) will react with NO_3 under our experimental conditions and can start a chain reaction, the length of which will determine the value of *s*.

Possible reactions that follow the abstraction of an allylic hydrogen in process (5) and that are fast enough at temperatures around 500 K to be operating in our system are

$$C_3H_5 + NO_3 \rightarrow C_3H_5ONO_2 \quad (7a)$$

$$\rightarrow C_3H_5O + NO_2 \quad (7b)$$

$$C_3H_5ONO_2 \rightarrow C_3H_5O + NO_2 \quad (8)$$

$$C_3H_5O \rightarrow C_2H_3 + HCHO \quad (9)$$

$$C_2H_3 + NO_3 \rightarrow \text{products } (C_2H_3O?) \quad (10)$$

$$HCHO + NO_3 \rightarrow HCO + HNO_3 \quad (11)$$

$$HCO + NO_3 \rightarrow \text{products} \quad (12)$$

$$HCO \rightarrow H + CO \quad (13)$$

$$C_3H_5 \rightarrow H + C_3H_4 \quad (14)$$

$$H + NO_3 \rightarrow OH + NO_2 \quad (15)$$

$$OH + NO_3 \rightarrow HO_2 + NO_2 \quad (16)$$

Reactions (8), (9), (13) and (14) have activation energies over 50 kJ mol^{-1}. Consequently, the stoicheiometry, *s*, for the abstraction channel could increase beyond two at elevated temperatures. For reaction (13), $\Delta_r H^0 \approx 70$ kJ mol^{-1}, and the rate coefficient could be *ca.* 2 s^{-1} at 500 K. However, for reaction (14), $\Delta_r H^0 \approx 240$ kJ mol^{-1}, and the process is unlikely to be a significant source of H atoms.

In order to estimate the values of *s* at $T = 473$ and 523 K, we must first evaluate the effect of the abstraction channel at the lower temperatures on the values of k_2 given in Table 1. Reactions (5) and (7)–(16) were included in our model in the form

$$CH_2{=}CHCH_3 + sNO_3 \rightarrow \text{products} \qquad (5')$$

For temperatures up to $T = 423$ K with $s = 2$, the values of k_5 calculated with eqn. (III) and employing the numerical model as outlined before, we obtained a set of 'corrected' values for k_2 which can be fitted by the expression

$$k_{2,\,\mathrm{corr}}/\mathrm{cm^3\ molecule^{-1}\ s^{-1}} = 2.04 \times 10^{-13} \exp[-(943 \pm 108)/T] \qquad (IV)$$

with a correlation coefficient of 0.995; the relation is shown in logarithmic form in Fig. 3. The activation energy would be 7.8 ± 0.8 kJ mol^{-1}, a value 20% lower than the one calculated from the uncorrected Arrhenius plot of Fig. 3.

We can now estimate the values of *s* for reaction (5′) at $T = 473$ and 523 K. Using eqn. (IV) we calculate $k_{2,\,\mathrm{corr}}$ as 2.8×10^{-14} and 3.4×10^{-14} cm^3 molecule^{-1} s^{-1}. At the same temperatures, eqn. (III) gives values for k_5 of 7.0×10^{-15} and 1.1×10^{-14} cm^3 molecule^{-1} s^{-1}. The model calculations were carried out including reactions (2), (3), (4) and (5′), and varying *s* by increments of 0.1. The deviation from the experimental data points was then calculated as before. The results are $s = 3.0$ at $T = 473$ K and $s = 4.0$ at 523 K, in agreement with the suggestion that the chain length increases with temperature.

The estimated Arrhenius parameters for the abstraction reaction [eqn. (III)] appear to be reasonable and they are consistent with our experimental data for propene as well as for other saturated and unsaturated hydrocarbons.[8,22,23] However, we recognize that there are assumptions made in deriving eqn. (III) and (IV); while we believe that the activation energy of 7.8 kJ mol^{-1} for the addition process is realistic, it must still be regarded as a lower limit, with the true value being possibly up to 20% greater. A comparison of the activation energies for the reactions of NO$_3$ with a series of organic compounds will be presented in a subsequent paper.[23]

Temperature-dependent *A* Factor

As pointed out earlier, curvature in the Arrhenius plot could conceivably exist even if only one channel operates. The temperature dependence of the rate constant can be expressed in the form

$$k = A'T^n \exp(-E'/RT) \qquad (V)$$

where *A*′ and *E*′ are related to the usual Arrhenius parameters *A* and *E* by the relations

$$A' = A(eT)^{-n} \qquad (VI)$$

$$E' = E - nRT \qquad (VII)$$

An estimate of *n* was obtained by the semi-empirical group-additivity method proposed by Benson[24] for the calculation of *A* factors as a function of temperature for the reaction of propene with NO$_3$ and using eqn. (VI); this approach leads to $n = 2.25$.[25,26] This value is not large enough to reproduce the curvature of the experimental Arrhenius plot in the range $T = 298$–523 K. According to Cohen,[27] for a reaction with a non-linear transition state, *n* should be in the range 0.5–4, but even with $n = 4$ the fit of the equation to the experimental data is poor. A very good fit to the experimental data can be obtained with $n = 12.9 \pm 1.3$,[25,26] but this value cannot have any physical significance.

We summarize now the reasons suggesting that the increasing importance with temperature of the secondary processes started by the abstraction of an allylic hydrogen is the most likely explanation for the curved Arrhenius plot. First, the Arrhenius plots for the reaction of NO$_3$ with alkanes (*n*- and iso-butane and iso-pentane), where abstraction is the only primary process, show the same upward curvature above $T = 423$ K.[22] Secondly, the Arrhenius plot for the reaction with ethene, where no abstraction channel is likely, is a good straight line up to $T = 523$ K.[8] Thirdly, the plots for the reactions with propyne, but-1-yne, pent-1-yne and hex-1-yne[8] are good straight lines from $T = 298$ to 473 and even 523 K. As we have indicated, there is evidence that the abstraction is much less favoured in the alkynes. Fourthly, a temperature-dependent pre-exponential factor fails to explain the curvature of the Arrhenius plot as just discussed. The Arrhenius plot for but-1-ene is a good straight line from $T = 298$ to 473 K.[23] This linearity is consistent with the suggestion that the contribution of the abstraction channel to the total reaction might be less for but-1-ene than for propene.

Atmospheric Implications

The main sources of propene in the atmosphere are oceanic emissions, microbial production in soils, biomass burning, emissions from foliage and engine exhaust. The atmospheric mixing ratios for propene vary from 0.2 to 0.5 ppb.[5] However, mixing ratios greater than 1 ppb have been found at sea level off the east coast of Africa.[6] An average atmospheric lifetime for propene of 15 h has been reported by Rudolph and Ehhalt.[28] Taking the atmospheric concentrations of OH by day as 10^6 molecule cm^{-3} and for NO$_3$ at night as 10^9 molecule cm^{-3} together with the rate constant for the reaction of propene with OH[16] (2.6×10^{-11} cm^3 molecule^{-1} s^{-1}) and k_2 from this work (0.93×10^{-14} cm^3 molecule^{-1} s^{-1}), we can estimate the daytime half-life of propene as 7.4 h and the half-life by night as 21 h. These values are consistent with the measurements of Rudolph and Ehhalt and indicate that roughly one-quarter of the atmospheric oxidation of propene can be ascribed to the reaction with NO$_3$. For a more precise figure, a knowledge of the regional and local variations in the concentrations of OH and NO$_3$ is needed.

We present now an example that illustrates the potential importance of the reaction of NO$_3$ with propene in heavily polluted air. In the presence of oxygen, a nitrated alkoxyl radical is formed. Although, under atmospheric conditions, this radical is likely[15] to decompose or react with oxygen, nevertheless one of the products of the reaction previously identified in smog chamber experiments is propylene glycol 1,2-dinitrate.[29] Overexposure to this compound is known to cause severe headaches, dizziness, eye irritation, vasomotor collapse and unconsciousness.[29,30] Such symptoms have been reported during severe smog episodes in the United States.[1]

The financial support of C.C-M. under research grants from the NERC and of S.J.S. by a studentship from the NERC is most gratefully acknowledged.

References

1 B. J. Finlayson-Pitts and J. N. Pitts Jr., *Atmospheric Chemistry*, Wiley, New York, 1986.
2 E. D. Morris Jr. and H. Niki, *J. Phys. Chem.*, 1974, **78**, 1337.
3 S. M. Japar and H. Niki, *J. Phys. Chem.*, 1975, **79**, 1629.
4 R. Atkinson, S. M. Aschmann and J. N. Pitts, Jr., *J. Phys. Chem.*, 1988, **92**, 3454.
5 J. Rudolph, *J. Geophys. Res.*, 1988, **93**, 67.
6 B. Bonsang, M. Kanakidou, G. Lambert and P. Monfray, *J. Atmos. Chem.*, 1988, **6**, 3.
7 C. E. Canosa-Mas, S. J. Smith, S. Toby and R. P. Wayne, *J. Chem. Soc., Faraday Trans. 2*, 1988, **84**, 247.
8 C. E. Canosa-Mas, S. J. Smith, S. Toby and R. P. Wayne, *J. Chem. Soc., Faraday Trans. 2*, 1988, **84**, 263.
9 E. J. Dlugokencky and C. J. Howard, *J. Phys. Chem.*, 1989, **93**, 1910.
10 G. Le Bras, V. Daele, I. T. Lançar, G. Laverdet, A. Mellouki and G. Poulet, CEC Project EV4V-0093-C, Final Report, 1991, Brussels.
11 C. A. Smith, A. R. Ravishankara and P. H. Wine, *J. Phys. Chem.*, 1985, **89**, 1423.
12 W. B. DeMore, S. P. Sander, D. M. Golden, M. J. Molina, R. F. Hampson, M. J. Kurylo, C. J. Howard and A. R. Ravishankara, *Chemical Kinetics and Photochemical Data for use in Stratospheric Modeling. Evaluation No. 9*, 1990, JPL Publication 90-1, Jet Propulsion Laboratory, Pasadena, Ca.
13 R. P. Wayne, I. Barnes, P. Biggs, J. P. Burrows, C. E. Canosa-Mas, J. Hjorth, G. Le Bras, G. K. Moortgat, D. Perner, G. Poulet, G. Restelli and H. Sidebottom, *Atmos. Environ.*, 1991, **25A**, 1.
14 H. Bandow, M. Okuda and H. Akimoto, *J. Phys. Chem.*, 1980, **84**, 3604.
15 P. B. Shepson, E. O. Edney, T. E. Kleindienst, J. H. Pittman and G. R. Namie, *Environ. Sci. Technol.*, 1985, **19**, 849.
16 R. Atkinson, *J. Phys. Chem. Ref. Data*, 1989, Monograph No. 1.
17 R. J. Cvetanovic and D. L. Singleton, *Rev. Chem. Intermed.*, 1984, **5**, 183.
18 K. Kleinermanns and A. C. Luntz, *J. Chem. Phys.*, 1982, **77**, 3533.
19 M. Rossi, K. D. King and D. M. Golden, *J. Am. Chem. Soc.*, 1979, **101**, 1223.
20 M. Rossi and D. M. Golden, *J. Am. Chem. Soc.*, 1979, **101**, 1230.
21 D. F. McMillen and D. M. Golden, *Annu. Rev. Phys. Chem.*, 1982, **33**, 493.
22 J. A. Bagley, C. E. Canosa-Mas, M. R. Little, A. D. Parr, S. J. Smith, S. J. Waygood and R. P. Wayne, *J. Chem. Soc., Faraday Trans.*, 1990, **86**, 2109.
23 C. E. Canosa-Mas, P. S. Monks and R. P. Wayne, in preparation.
24 S. W. Benson, *Thermochemical Kinetics*, Wiley, New York, 1976.
25 S. J. Waygood, Part II Thesis, University of Oxford, 1988.
26 C. E. Canosa-Mas, S. J. Smith, S. J. Waygood and R. P. Wayne, *Tenth International Symposium on Gas Kinetics*, paper A45, University College of Swansea, 1988.
27 N. Cohen, *Tenth International Symposium on Gas Kinetics*, paper A43, University College of Swansea, 1988, and personal communication, 1988.
28 J. Rudolph and D. H. Ehhalt, *J. Geophys. Res.*, 1981, **86**, 11959.
29 H. Akimoto, M. Hoshino, G. Inoue, M. Okuda and N. Washida, *Bull. Chem. Soc. Jpn.*, 1978, **51**, 2496.
30 E. C. Tuazon, E. Sanhueza, R. Atkinson and W. P. L. Carter, *J. Phys. Chem.*, 1984, **88**, 1210.

Paper 1/03420K; *Received* 8*th July*, 1991